MITSUBISHI ELECTRIC RESEARCH LABORATORIES
http://www.merl.com

Ranging in the IEEE 802.15.4a Standard

Zafer Sahinoglu, Sinan Gezici

TR2006-097   December 2006

Abstract

The emerging IEEE 802.15.4a standard is the first international standard that specifies a wireless physical layer to enable precision ranging. In this article, ranging signal waveforms and ranging protocols adopted into the standard are discussed in a tutorial manner.

IEEE Wireless and Microwave Technology Conference (WAMICON)

Ranging in the IEEE 802.15.4a Standard

Zafer Sahinoglu and Sinan Gezici
Mitsubishi Electric Research Laboratories
201 Broadway, Cambridge, MA 02139, USA
Email: {zafer, gezici}@merl.com

(Invited Paper)

***Abstract*— The emerging IEEE 802.15.4a standard is the first international standard that specifies a wireless physical layer to enable precision ranging. In this article, ranging signal waveforms and ranging protocols adopted into the standard are discussed in a tutorial manner.**

***Index Terms*— Radio range measurements, ultra-wideband (UWB), IEEE 802.15.4a standard.**

I. Introduction

Short-range wireless sensor network applications are becoming increasingly popular [1], [2]. The IEEE 802.15.4 and ZigBee standards are results of a continuously growing market demand for such applications, many of which require location-awareness [3]. Due to the importance of location-awareness in wireless networks, the IEEE 802.15.4a Task Group (TG) has developed an ultra-wideband (UWB) based physical layer standard for short-range networks with a precision ranging capability [4].

The IEEE 802.15.4a specifies two optional signalling formats based on impulse radio (IR) UWB and chirp spread spectrum (CSS). The IR-UWB system can use 250-750 MHz, 3.244-4.742 GHz, or 5.944-10.234 GHz bands; whereas the CSS uses the 2.4-2.4835 GHz band. For the IR-UWB option, there is an optional ranging capability, whereas the CSS signals can only be used for data communication [4]. Since we investigate ranging for the IEEE 802.15.4a standard in the present paper, we only focus on the IR-UWB option of the standard.

An IR-UWB system employs very narrow pulses to transmit information, which is usually conveyed by the positions and/or polarities of the pulses [5]-[10]. Unlike the conventional IR-UWB systems, the information is conveyed by the positions and polarities of *pulse bursts* in the IEEE 802.15.4a standard [4]. In other words, the signalling structure in the payload field of an IEEE 802.15.4a packet is a modified version of the classical IR-UWB signalling. However, for the synchronization preamble of the packet, UWB pulses with a low duty cycle are transmitted similarly to a classical IR-UWB system. Since the preamble is the part of the IEEE 802.15.4a packet that is used for ranging purposes, we will focus on the preamble section when investigating the ranging issues.

In this paper, we investigate the UWB physical layer (PHY) of the IEEE 802.15.4a standard from a ranging point of view. For that purpose, we first look at the design of the IEEE 802.15.4a packet structure and discuss its advantages for ranging. Then, we analyze the ranging protocols specified in the standard including mandatory and optional protocols, and the enhancements for ranging privacy.

The remainder of the paper is organized as follows. In section II, basics of ranging and related terminology are introduced. Then, the IEEE 802.15.4a packet structure is investigated from a ranging point of view in section III. Finally, ranging protocols are studied in section IV, which is followed by the concluding remarks in the last section.

II. Basics of Ranging

According to the IEEE 802.15.4a terminology, *RDEV* is called the ranging capable device, which implements the optional ranging support, and *RFRAME* is the ranging frame. The *RFRAME* is indicated by setting a ranging bit in the PHY header of the IEEE.802.15.4a packet. A range between two *RDEV*s is determined typically via two-way exchange of an *RFRAME* and tracking its arrival time as illustrated in Figure 1. This is called two-way time-of-arrival (TW-TOA). Assume that *RDEV A* wants to perform ranging with *RDEV B*. The elapsed time between the departure of *RFRAME* from *A* and the reception of the reply *RFRAME* from *B*, T_r, can be approximated as $T_r = 2T_t + T_{ta}$, where T_t is the one-way time of flight of the first arriving signal component and T_{ta} is the turn-around time.

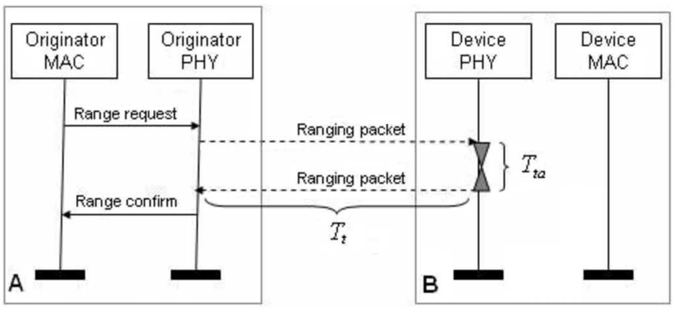

Fig. 1. Message exchanges in two-way time of arrival based ranging.

The ranging performance depends on how accurately T_t can be estimated. For a single path additive white Gaussian noise (AWGN) channel, the Cramer-Rao lower bound for the variance of the time-of-flight estimate $\hat{T}_t$ is expressed as $\sqrt{\mathrm{Var}(\hat{T}_t)} \geq \left(2\sqrt{2}\pi\sqrt{\mathrm{SNR}}\beta\right)^{-1}$, where SNR is the signal-to-noise ratio and β is the effective signal bandwidth [11]. Apparently, high SNR and/or wider bandwidth help reduce the range error.

UWB signals have relative bandwidths of more than 20% or absolute bandwidths of at least 500 MHz [12]. This large bandwidth provides high time resolution and facilitates better detection of leading signal edge. Also, the probability of some frequency components penetrating through or going around an obstacle increases. Therefore, it becomes more likely to encounter a line-of-sight (LOS) signal. In other words, both high resolution and penetration capability make UWB signals suitable for ranging purposes.

Similar to other wireless geolocation systems, the main sources of ranging errors in UWB ranging systems are multipath propagation, non-line-of-sight (NLOS) propagation and multi-user interference (MUI) [13]. In highly scatter environments, multiple copies of a transmitted signal with various attenuation levels and time-delay arrive at a receiver. Therefore, match filtering or correlation-based TOA processing would return multiple peaks, while only the time of the first peak is significant for precision ranging. When the direct LOS between ranging nodes is obstructed or multiple reflections from scatterers superpose, the first peak may not be the strongest one [14], [15].

In the IEEE 802.15.4a standard, the packet preamble is designed in consideration of multipath channels so as to make first path detection easier. However, implementation of a leading edge search engine is still required [16]-[19].

III. IEEE 802.15.4a Packet Structure

In IEEE 802.15.4a networks, devices communicate using the packet format illustrated in Figure 2. The IEEE 802.15.4a packet consists of a synchronization header (SHR) preamble, a physical layer header (PHR) and a data field. The SHR preamble is composed of the (ranging) preamble and the start of frame delimiter (SFD), which are investigated in the following subsections.

A. Preamble

The number of symbols in the ranging preamble are specified according to application requirements. There can be 16, 64, 1024 or 4096 symbols in the preamble depending on the channel power delay profile, the SNR of the link and capabilities of *RDEV*s. The longer lengths, 1024 and 4096, are preferred for non-coherent receivers to help them improve the SNR via processing gain. Hence, they can have a reasonably accurate TOA estimate.

It is suggested in the standard that the application should start ranging operations by setting the preamble length to 1024 symbols. By keeping track of the reported *figure-of-merits* (FoMs)[1], future adjustments to the preamble length can be made.

The underlying symbol of the ranging preamble uses one of the length-31 ternary sequences, $\mathbf{S}_i$, in Table I. Each $\mathbf{S}_i$ of length $L = 31$ contains 15 zeros and 16 non-zero codes, and

[1]As the acquisition is achieved earlier in the preamble, the receiver finds a better opportunity to refine its leading edge timing estimate. This is quantified in the standard by a parameter so-called *figure-of-merit* (FoM), and it is reported to the position solver, which resides above the MAC layer.

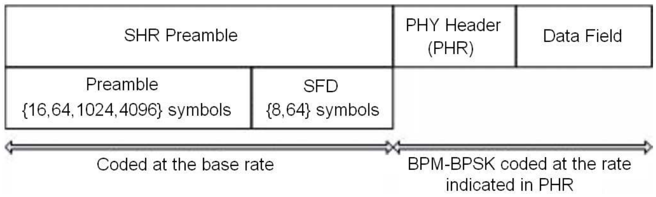

Fig. 2. Illustration of the IEEE 802.15.4a packet structure (BPM-BPSK: Burst Position Modulation-Binary Phase Shift Keying).

has the much desired property of perfect periodic autocorrelation. In other words, the side-lobes of their periodic correlation are zero (Figure 3); and what is observed at the receiver between two consecutive correlation peaks becomes only the power delay profile of the channel. Thus, the TOA detection performance does not get deteriorated by autocorrelation side-lobes.

TABLE I
THE BASIS PREAMBLE SYMBOL SET

Index	Symbol
$\mathbf{S}_1$	-0000+0-0+++0+-000+-+++00-+0-00
$\mathbf{S}_2$	0+0+-0+0+000-++0-+—00+00++000
$\mathbf{S}_3$	-+0++000-+-++00++0+00-0000-0+0-
$\mathbf{S}_4$	0000+-00-00-++++0+-+000+0-0++0-
$\mathbf{S}_5$	-0+-00+++-+000-+0+++0-0+0000-00
$\mathbf{S}_6$	++00+00—+-0++-000+0+0-+0+0000
$\mathbf{S}_7$	+0000+-0+0+00+000+0++—0-+00-+
$\mathbf{S}_8$	0+00-0-0++0000–+00-+0++-++0+00

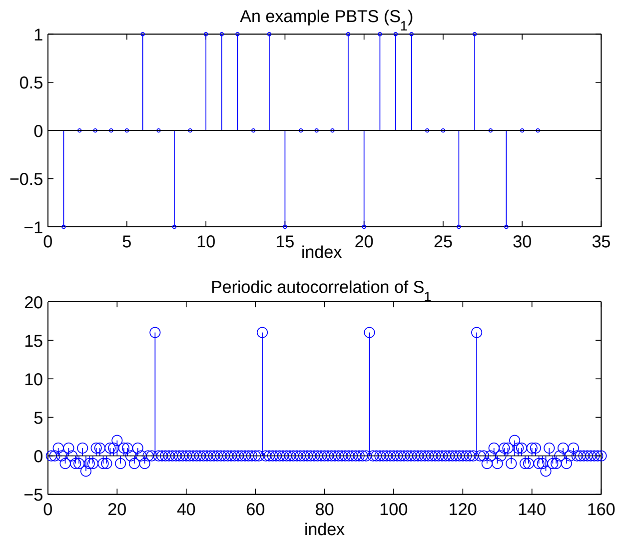

Fig. 3. Illustration of a perfectly balanced ternary sequence (PBTS) for the IEEE 802.15.4a standard and its periodic autocorrelation.

Assume that $\phi(t)$ is the transmitted UWB pulse waveform with unit energy, $T_{\rm sym}$ denotes the symbol duration, $N_{\rm sym}$ is the number of symbol repetitions within the preamble, $T_{\rm pri}$ is the pulse repetition interval, $N_{\rm s}$ is the total number of pulses per symbol and $E_{\rm s}$ is the symbol energy. Then, for the ith basis symbol $\mathbf{S}_i$, the preamble symbol waveform $w_i(t)$ and the resulting preamble waveform $P_i(t)$ can be written as

$$w_i(t) = \sqrt{\frac{E_\mathrm{s}}{N_\mathrm{s}}} \sum_{j=0}^{L-1} \mathbf{S}_i[j]\phi\big(t - jT_\mathrm{pri}\big), \tag{1}$$

$$P_i(t) = \sum_{n=0}^{N_\mathrm{sym}-1} \mathbf{N}[n] w_i(t - nT_\mathrm{sym}), \tag{2}$$

where $\mathbf{S}_i[j]$ denotes the jth element of $\mathbf{S}_i$, and $\mathbf{N} = [1\ 1 \cdots 1]_{1 \times N_\mathrm{sym}}$.

In [20], it is suggested that for non-coherent detection of a ternary sequence $\mathbf{S}_i$, the optimum template is its bipolar form, that is $2|\mathbf{S}_i| - 1$. This mismatched template correlation also preserves the perfect periodic autocorrelation property of the PBTS sequences in Table I.

B. SFD

The SFD signals the end of the preamble and the beginning of the PHY header. In other words, it is used to establish frame timing; and its detection is important for accurate counting of the turn around time T_{ta} and also for computing the FoM. It can consist of 8 or 64 symbols. The IEEE 802.15.4a PHY supports a mandatory short SFD (8 symbols) for default (1 Mbps) and medium data rate and an optional long SFD (64 symbols) for the nominal low data rate of 106 Kbps.

Let $\mathbf{M}$ denote a vector of ternary codes $\{-1, 0, +1\}$ and assume that its length is equal to the number of symbols in the SFD, L_sfd. Then, the SFD waveform $Z_i(t)$ is generated by spreading the so-called outer sequence $\mathbf{M}$ with the basis symbol $\mathbf{S}_i$, that is the inner sequence:

$$Z_i(t) = \sum_{m=0}^{L_\mathrm{sfd}-1} \mathbf{M}[m] w_i(t - mT_\mathrm{sym}), \tag{3}$$

where $w_i(t)$ is as in (1). Then, the entire SHR preamble waveform $Y_i(t)$ can be expressed as

$$Y_i(t) = P_i(t) + Z_i(t - N_\mathrm{sym}T_\mathrm{sym}), \tag{4}$$

where $P_i(t)$ is given by (2).

Assume that $\mathbf{M}_l$ and $\mathbf{M}_s$ indicate the outer sequences for long and short SFDs, respectively. They should have the following key properties.

Property-I: $\mathbf{M}_l[k] = \mathbf{M}_s[k], 0 \leq k \leq 7$. The correlation template for SFD detection in high data rate receivers should be equal to the short SFD. Making the first eight codes of $\mathbf{M}_l$ and $\mathbf{M}_s$ the same spares the high data rate receivers from running two separate correlators to distinguish the short and long SFDs.

Property-II: $\mathbf{M}_l[k] = \mathbf{M}_l[k+8], 0 \leq k \leq 7$. By exploiting this feature, the high data rate receiver can identify the long SFD, because its correlation output fires twice while receiving the short SFD, due to repetition of the first eight codes of $\mathbf{M}_l[k]$. Hence, after the second firing, the correlation can stop.

Property-III: $\sum_{k=0}^{7} \mathbf{M}_l[k] = 0$ and $\sum_{k=0}^{7} \mathbf{M}_s[k] = 0$. The first eight codes in $\mathbf{M}_l$ and $\mathbf{M}_s$ should be balanced. Therefore, when the correlation window is running through the preamble, its output becomes zero. Thus, the transition of the correlation from preamble into the SFD is prevented from degrading the detection of the SFD.

After an exhaustive search, a long SFD sequence that satisfies the above three properties is found (Table II), which is standardized by the IEEE 802.15.4a TG. Note that the corresponding short SFD sequence $\mathbf{M}_s$ is simply the first 8 elements of $\mathbf{M}_l$.

TABLE II
THE LONG SFD SEQUENCE

Index	Sequence (length-64)
$\mathbf{M}_l$	0+0-+00-0+0-+00–00+0-0+0+000-0- 0-00+0–0-+0000++00—+-++0000++

In Table III, the properties of the long and short SFD sequences are investigated in terms of peak-to-maximum sidelobe (PMSL) and peak-to-average sidelobe (PASL) ratios for both coherent and non-coherent structures.

IV. RANGING PROTOCOLS

The standard adopts a slightly modified version of the conventional two way ranging protocol as mandatory. Moreover, by symmetric double-sided *RFRAME* two-way signal exchanges, it is also possible to eliminate clock offset differences between the *RDEV*s. Both these protocols estimate the range without a common timing reference. In some applications, the range information is a critical deliverable. Therefore, the standard also supports private ranging to safeguard the integrity of the ranging traffic itself. In what follows, we provide details of these ranging protocols.

A. Mandatory Ranging Protocol

The mandatory ranging protocol is *TW-TOA*, which only mandates the transmission of D_2, A_2, D_4 and A_4 in Figure 4. First, the originator *RDEV A* sends a range request packet D_2 and the recipient *RDEV B* replies with an acknowledgment A_2. The recipient also transmits a time-stamp packet, D_4, following the transmission of A_2. Finally, *RDEV A* sends an acknowledgement, A_4, for the time stamp.

1) Time-stamp Report: There are five parameters that characterize a single range measurement and form the time-stamp report: ranging counter start value, ranging counter stop value, two numbers to characterize the crystals and FoM. There is a total of 16 octets in a time-stamp report. These values are generated by the PHY as a set, and not split apart during subsequent data handling.

TABLE III
PEAK-TO-MAXIMUM SIDELOBE (PMSL) AND PEAK-TO-AVERAGE SIDELOBE (PASL) LEVELS (IN dB) OF THE LONG AND SHORT SFD SEQUENCES.

	Coherent		Non-coherent	
	PMSL	PASL	PMSL	PASL
$\mathbf{M}_l$	7.27	17.6	8.06	20.9
$\mathbf{M}_s$	6.02	13.2	6.02	18.0

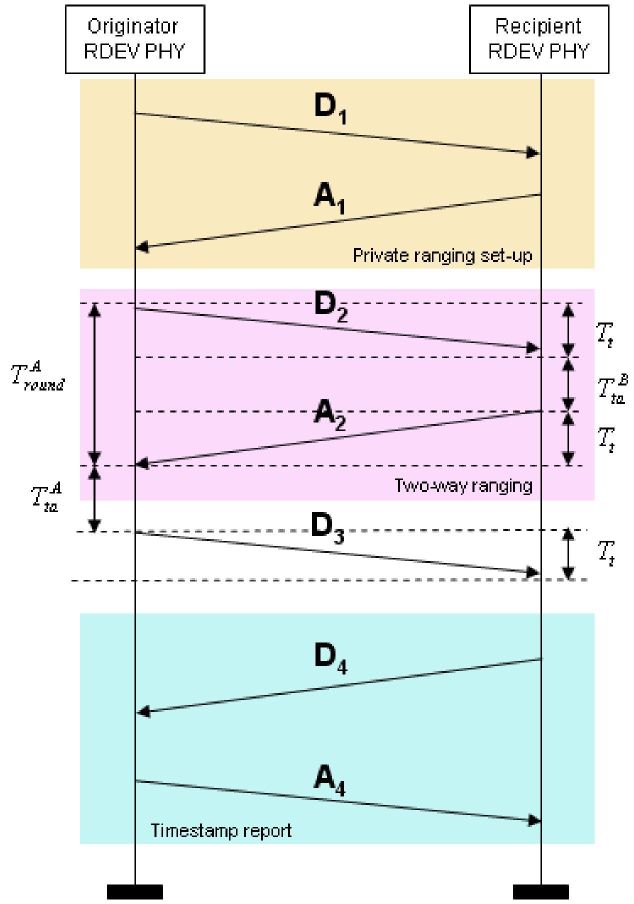

Fig. 4. Illustration of the ranging protocols supported by the IEEE 802.15.4a standard

The counter start value represents the TOA of the first pulse of the first symbol of the PHR. The ranging counter start and stop values are reported with 4 octets each. Even though the real use is their difference, the IEEE 802.15.4a standard PHY handles them separately. One strong reason is to allow flexibility for an infrastructure based time-difference-of-arrival implementation, which is not concerned about the start time.

Assume that *B* detects the *SFD* marker of D_2 according to its own clock at t_{b1} and also records the time when the *SFD* marker of A_2 leaves *B*'s antenna at t_{b2}. Then, the time-stamp report should contain both t_{b1} and t_{b2} as the counter start and stop values.

An *RDEV* that implements the optional crystal characterization produces a tracking offset and a tracking interval. The tracking offset is a signed magnitude integer. The value of the integer is a number that represents the difference in frequency between the receiver's oscillator and the transmitter's oscillator after the tracking offset integer is divided by the tracking interval integer. For example, if the difference between the oscillators is ten parts per million, then an acceptable value of the ranging tracking offset would be ten when the ranging tracking interval is 1 million.

Finally, the *FoM* characterizes the accuracy of the *PHY* estimate of the arrival time of the leading edge of the first pulse of the *PHR* at the antenna. The *FoM* is composed of 3 subfields and an extension bit. The confidence level sub-field indicates the confidence level of the range measurement in 3 bit allocation for a given confidence interval. The confidence interval can be any of 100 ps, 300 ps, 1 ns and 3 ns. The FoM confidence interval scaling factor is used to set the confidence interval to some intermediate values.

B. Optional Symmetric Double Sided (SDS) TW-TOA Protocol

The double symmetric ranging protocol [21] is illustrated with messages D_2, A_2, D_3 in Figure 4. Addition of D_3 to the TW-TOA reduces the effect of the finite crystal tolerances e_A and e_B of the originator and target *RDEV*s, respectively.

It is clear from Figure 4 that

$$T_t = \frac{1}{4}\left(T^A_{round} - T^A_{ta} + T^B_{round} - T^B_{ta}\right). \qquad (5)$$

After factoring in the crystal tolerances, the estimate for T_t becomes

$$\hat{T}_t^{\text{SDS}} = \frac{1}{4}\Big(\left(T^A_{round} - T^A_{ta}\right)(1+e_A) + \left(T^B_{round} - T^B_{ta}\right)(1+e_B)\Big). \qquad (6)$$

Assuming that $T^B_{ta} = T^A_{ta} + \delta$ and $T_t \ll \delta$, $\hat{T}_t^{\text{SDS}}$ in (6) can be approximately expressed as

$$\hat{T}_t^{\text{SDS}} \approx T_t + \frac{1}{4}\delta(e_A - e_B), \qquad (7)$$

whereas in the TW-TOA, it is shown in [21] that

$$\hat{T}_t^{\text{TW}} \approx T_t + \frac{1}{2}\delta(e_A - e_B). \qquad (8)$$

The comparison of (7) with (8) reveals that the *SDS-TW-TOA* results in a considerably smaller error margin than *TW-TOA*.

C. Optional Private Ranging Protocol

Ranging is very useful in sensor networks, but can be subject to hostile attacks especially in security-related networks. A number of attacks is possible:

- *Snooper attack:* A hostile device listens to ranging exchanges, and tries to determine positions of the *RDEV*s.
- *Impostor attacks:* A hostile device transmits a conventional *RFRAME* for originating, and targets *RDEV*s so as to confuse their acquisition timing.
- *Jamming attack:* A hostile device jams during transmission of *RFRAME*s to entirely harm acquisition and ranging.

In order to make such attacks more difficult, the IEEE 802.15.4a standard foresees a "private ranging" mode. In this mode, the ranging preamble uses one of length 127 PBTS given in Table IV.

The nodes exchange via a secure protocol the sequences to be used in the next ranging cycle. This prevents impostor attacks, and makes snooper attacks more difficult (a snooper now has to listen to 8 possible ranging waveforms). Private ranging is provisioned in two steps: *authentication* and *ranging*.

TABLE IV

THE PREAMBLE SYMBOL SET FOR PRIVATE RANGING

Index	Symbol
P_1	+000–0000–++0-++++0-0++0+0-00-+0++00++-0 ++0+-+0-00+00-0–000-+-00+0000-0++-00000+-0 -000000-00-+-++-+000-0+0+0+++-00–00+0+000
P_2	+000++0-0+0-00+-0-+0-00+0+0000+0+-0000++00 +0+++++-+0-0+-0–+0++–000—0+000+0+0-+-00 0000+-+-0–00++000-00+00++-00–++-00-00000
P_3	0+-00+0-000-++0000—++000+0+-0-+00-+000– 0-00–0–+++-+0-++00+-++0+00000+0-0+++-00+0 0+000-0000+00–+0++0+0+0-00-0-+-0+0++00000
P_4	++0000+000+00+–0+-++0-000–00+-0+00++000+ ++00+0+0-0-+-0-0+00+00+0++—-+00++–+0+-0- -+000000-0-0000-+0–00+00000+-++000-0-+0+0
P_5	+0+00–00-+++0+0+0-000+-++-+-00-000000-0-+ 00000-++0-0000+00-+-000–0-00+00-0+-+0++0-+ +00++0+-00-0+0++0-0++++-0++–0000–000+000
P_6	0-00-++–00-++00+00-000++00–0-+-+000000-+ -0+0+000+0—000–++0+–0-+0-0+-+++++0+00++ 0000-+0+0000+0+00-0+-0-+00-0+0-0++000+0000
P_7	000++0+0-+-0-00-0+0+0++0+–00+0000-000+00+ 00-+++0-0+00000+0++-+00++-0+-+++–0–00-0– 000+-00+-0-+0+000++—0000++-000-0+00-+000
P_8	+0+-0-000++-+00000+00–0+-0000-0-000000+– 0-+0+–++00+—-++0+00+00+0-0-+-0-0+0+00+++ 000++00+0-+00–000-0++-+0–+00+000+0000++0

1) Authentication Phase: First, the originator *RDEV* (A) should send a so-called *range authentication packet* (RAP) to the target *RDEV* (B). This packet is shown as D_1 in Figure 4. The main purpose of the RAP is first to ensure that the originator device is authentic, and second to convey, in its encrypted payload, identifiers of the two length-127 preamble symbols $DPS_{\rm tx}$ and $DPS_{\rm rx}$ to be used in the *RFRAMES* D_2 and A_2, respectively. The $DPS_{\rm tx}$ and $DPS_{\rm rx}$ are randomly selected from Table IV. If *B* finds *A* authentic, it may reply with an ACK (A_1). This high layer authentication helps to interdict impostors.

The $DPS_{\rm tx}$ and $DPS_{\rm rx}$ should be varied for each ranging process to deal with replay attacks. Probability of picking the right $DPS_{\rm tx}$ or $DPS_{\rm rx}$ for a malicious device goes down to $1/8$ from 1. The *RAP* might seem to be an overhead for the benefit of privacy. However, if the originator is performing ranging with all its N neighbors, a single broadcast RAP might be sufficient.

2) Ranging Phase: During the ranging phase, *RDEV A* transmits *RFRAME* D_2 that uses $DPS_{\rm tx}$ as its preamble symbol; and in return *RDEV B* sends back an *ACK* A_2, of which the underlying preamble symbol is $DPS_{\rm rx}$. Finally, the time-stamp report D_4 and acknowledgement A_4 by the originating *RDEV* completes the private ranging protocol.

Encrypting time-stamp reports proves to be an effective technique to keep hostile devices from learning range information. As the reports are moved after the time critical ranging exchange is complete, the encryption does not become time sensitive.

V. CONCLUSIONS

In this tutorial paper, we have presented the issues related to ranging capability in the IEEE 802.15.4a standard. The design criteria for the preamble and SFD fields of the packets have been discussed. Ranging protocols supported by the standard have been explained, including TW-TOA, SDS-TW-TOA and private ranging protocols.

REFERENCES

[1] I. F. Akyildiz, W. Su, Y. Sankarasubramaniam and E. Cayirci, "A survey on sensor networks," *IEEE Communications Magazine,* vol. 40, issue 8, pp. 102-114, Aug. 2002.

[2] T. Arampatzis, J. Lygeros and S. Manesis, "A survey of applications of wireless sensors and wireless sensor networks," *Proc. 13th Mediterranean Conference on Control and Automation,* pp. 719-724, Limassol, Cyprus, June 27-29, 2005.

[3] ZigBee Alliance, [Online]. Available: http://www.zigbee.org

[4] IEEE P802.15.4a/D4 (Amendment of IEEE Std 802.15.4), "Part 15.4: Wireless Medium Access Control (MAC) and Physical Layer (PHY) Specifications for Low-Rate Wireless Personal Area Networks (LRW-PANs)," July 2006.

[5] M. Z. Win and R. A. Scholtz, "Impluse radio: How it works," *IEEE Communications Letters,* 2(2): pp. 36-38, Feb. 1998.

[6] M. Z. Win and R. A. Scholtz, "On the energy capture of ultra-wide bandwidth signals in dense multipath environments," *IEEE Communications Letters,* vol. 2, pp. 245-247, Sep. 1998.

[7] M. L. Welborn, "System considerations for ultra-wideband wireless networks," *Proc. IEEE Radio and Wireless Conference,* pp. 5-8, Boston, MA, Aug. 2001.

[8] R. A. Scholtz, "Multiple access with time-hopping impulse modulation," *Proc. IEEE Military Communications Conference, 1993 (MILCOM'93),* vol. 2, pp. 447-450, Bedford, MA, Oct. 1993.

[9] M. Z. Win and R. A. Scholtz, "Ultra-wide bandwidth time-hopping spread-spectrum impulse radio for wireless multiple-access communications," *IEEE Transactions on Communications,* vol. 48, issue 4, pp. 679-691, Apr. 2000.

[10] S. Gezici, H. Kobayashi, H. V. Poor and A. F. Molisch, "Performance evaluation of impulse radio UWB systems with pulse-based polarity randomization in asynchronous multiuser environments," *Proc. IEEE Wireless Communications and Networking Conference (WCNC 2004),* vol. 2, pp. 908-913, Atlanta, GA, March 21-25, 2004.

[11] H. V. Poor, *An Introduction to Signal Detection and Estimation,* Springer-Verlag, New York, 1994.

[12] U. S. Federal Communications Commission, "First Report and Order 02-48," Washington, DC, 2002.

[13] S. Gezici, Z. Tian, G. B. Giannakis, H. Kobayashi, A. F. Molisch, H. V. Poor and Z. Sahinoglu, "Localization via UWB Radios," *IEEE Signal Processing Magazine,* vol. 22, no. 4, pp. 70-84, July 2005.

[14] S. Gezici, Z. Sahinoglu, H. Kobayashi and H. V. Poor, "Ultra wideband geolocation". In H. Arslan, Z. N. Chen and M.-G. Di Benedetto, editors, *Ultra Wideband Wireless Communications,* Wiley-Interscience, Oct. 2006.

[15] A. F. Molisch, "Status of channel modeling-Final report," *IEEE P802.15-04-0662-01-004a/r0,* March 2005 [Online]. Available: http://802wirelessworld.com

[16] J-Y. Lee and R. A. Scholtz, "Ranging in a dense multipath environment using an UWB radio link," *IEEE Transactions on Selected Areas in Communications,* vol. 20, no. 9, pp. 1677-1683, Dec. 2002.

[17] L. Yang and G. B. Giannakis, "Blind UWB timing with a dirty template," *Proc. IEEE International Conference on Acoustics, Speech and Signal Processing*, Montreal, Quebec, Canada, May 17-21, 2004.

[18] W. C. Chung and D. S. Ha, "An accurate ultra wideband (UWB) ranging for precision asset location," *Proc. IEEE Conference on Ultra Wideband Systems and Technologies (UWBST'03)*, pp. 389-393, Reston, VA, Nov. 2003.

[19] S. Gezici, Z. Sahinoglu, A. F. Molisch, H. Kobayashi and H. V. Poor, "A two-step time of arrival estimation algorithm for impulse radio ultra-wideband systems," *Proc. 13th European Signal Processing Conference,* Antalya, Turkey, Sept. 4-8, 2005.

[20] F. Chin *et. al.* "Impulse radio signalings for communication and ranging", *IEEE 802.15.4a standard, doc. no. 15-05-0231-07-004a,* July 2005.

[21] R. Hach, "Symmetric double sided two-way ranging," *IEEE 802.15.4a standard, doc. IEEE P.802.15-05-0334-00-004a,* June 2005.